An EDQNM study of the dissipation rate in isotropic non-equilibrium turbulence

Le Fang, Wouter J.T. Bos

Journal of Turbulence

ISSN: (Print) (Online) Journal homepage: https://www.tandfonline.com/loi/tjot20

An EDQNM study of the dissipation rate in isotropic non-equilibrium turbulence

Le Fang & Wouter J.T. Bos

To cite this article: Le Fang & Wouter J.T. Bos (2023) An EDQNM study of the dissipation rate in isotropic non-equilibrium turbulence, Journal of Turbulence, 24:6-7, 217-234, DOI: 10.1080/14685248.2023.2189731

To link to this article: https://doi.org/10.1080/14685248.2023.2189731

JOURNAL OF TURBULENCE
2023, VOL. 24, NOS. 6–7, 217–234
https://doi.org/10.1080/14685248.2023.2189731

Taylor & Francis
Taylor & Francis Group

An EDQNM study of the dissipation rate in isotropic non-equilibrium turbulence

Le Fang[a,b] and Wouter J.T. Bos[c]

[a]LCS, Ecole Centrale de Pékin, Beihang University, Beijing, People's Republic of China; [b]Beihang Hangzhou Innovation Institute Yuhang, Hangzhou, People's Republic of China; [c]Univ Lyon, École Centrale de Lyon, INSA Lyon, Université Claude Bernard Lyon 1, CNRS, Laboratoire de Mécanique des Fluides et d'Acoustique, UMR 5509, Ecully, France

ABSTRACT

The energy cascade from large to small scales is a robust feature of three-dimensional turbulence. In statistically steady turbulence, the average dissipation is in equilibrium with the energy injected in the system. A global quantity measuring the deviations from such a flux equilibrium is the normalised dissipation rate C_ϵ, corresponding to the viscous dissipation, normalised by quantities associated with the largest scales of the system. Recent investigations have pointed out how this normalised dissipation rate varies in unsteady flows. We focus on two test-cases to assess non-equilibrium in isotropic turbulence. These cases are, respectively, turbulence in the presence of a large-scale periodic forcing and turbulence with reversed initial conditions. We show, using the Eddy-Damped Quasi-Normal Markovian closure, that for turbulence in the presence of periodic forcing, a $C_\epsilon \sim R_\lambda^{-15/14}$ scaling is reproduced (R_λ indicating the Taylor-scale Reynolds number) when the forcing-frequency is adjusted to be of the order of the inverse of the integral time-scale. It is shown that the spectrum can be decomposed into an equilibrium spectrum, governed by Kolmogorov scaling in the inertial range, and a perturbation spectrum, proportional to $k^{-7/3}$, k being the wavenumber. For reversed turbulence, a novel procedure is introduced to prescribe initial conditions for the nonlinear transfer. Subsequently a clear transient with a scaling $C_\epsilon \sim R_\lambda^{-2}$ is observed in the dynamics.

ARTICLE HISTORY
Received 18 November 2022
Accepted 21 February 2023

KEYWORDS
Isotropic turbulence; EDQNM; non-equilibrium

1. Introduction

1.1. Non-equilibrium and the normalised dissipation rate

One of the principle features of turbulence is its multiscale nature. In order to characterise a turbulent flow one needs to describe the statistics resulting from the interaction of a large number of scales. In most applications, where the knowledge of the detailed features of individual scales is unimportant, it is useful to have a simple relation which connects the dynamics of the different scales in a global way. This marks the importance of Taylor's

CONTACT Wouter J. T. Bos wouter.bos@ec-lyon.fr Univ Lyon, École Centrale de Lyon, INSA Lyon, Université Claude Bernard Lyon 1, CNRS, Laboratoire de Mécanique des Fluides et d'Acoustique, UMR 5509, 36 Avenue Guy de Collongue, F-69134 Ecully, France

relation [1],

$$\epsilon = C_\epsilon \frac{U^3}{L}. \tag{1}$$

In this relation ϵ is the dissipation rate of kinetic energy, in essence a small scale feature, and U and L are characteristic velocity and lengthscales, associated with the large, energy containing scales of the flow. This relation links therefore, by introducing a proportionality parameter C_ϵ, the dynamics of large and small scales. The quantity $C_\epsilon \equiv \epsilon L/U^3$, or normalised dissipation rate, can be considered the corner-stone of turbulence modeling and the assumption that it is constant is implicitly used in the majority of turbulence models, since it allows to express the dissipation scales by the information at scale L. For this constancy to hold, some kind of equilibrium must be assumed between the large and the small scales. The notion of equilibrium is a delicate one in a non-equilibrium system such as turbulence [2] and it is this notion of equilibrium, and its influence on the normalised dissipation, that we will focus on.

Given its importance in turbulence modeling, it is not surprising that expression (1) has received considerable attention. Early experimental results on its Reynolds number dependence are reported by Sreenivasan [3] and it was shown that for high Reynolds numbers C_ϵ tends to a constant value of order unity. In the 2000s it was realised that the value of C_ϵ might not be universal and that L, U and ϵ should be carefully defined [4,5]. Even in isotropic turbulence the value of C_ϵ can vary and it was shown that statistically stationary and freely decaying flows yield different values, which can be explained by the intrinsic imbalance between large and small scales in freely decaying turbulence [6]. A link was also found between the value of the normalised dissipation rate and the stagnation-points in a flow [7].

The investigation of C_ϵ revived after measurements [8–10] which showed that when turbulence statistics are evaluated near a grid placed in a wind-tunnel, C_ϵ is not constant, but evolves as a function of the Taylor-scale Reynolds number (defined below), approximately proportional to R_λ^{-1}. Far enough beyond the grid, a constant value is found for C_ϵ [10], as classically expected. Note that these observations of non-constant normalised dissipation persist at high enough values of the Reynolds number to discard low-Reynolds number corrections as an explanation. The same relation ($C_\epsilon \sim R_\lambda^{-n}$, with $n \approx 1$) was also observed to describe fluctuations around a steady state in the very controlled framework of periodic-box turbulence [11] and using a closure model [12].

No satisfactory explanation was obtained until it was shown that the non-equilibrium dissipation scaling can be derived analytically [13] using an existing form of a non-equilibrium correction to Kolmogorov's energy spectrum [14], proportional to $k^{-7/3}$, with k the wavenumber. This showed that the observed non-equilibrium scaling of C_ϵ is the consequence of the shape of the perturbation spectrum. This yields for the normalised dissipation rate a scaling proportional to $R_\lambda^{-15/14}$, a functional form very close to, and given the size of errorbars not easily distinguishable from the observed R_λ^{-1} scaling in simulations and experiments.

In a subsequent investigation [15] it was shown that in grid-turbulence, the region where this scaling is observed coincides with the part of the flow where the shear-layers, generated by the grid, are still present. Clearly, in this region, strong coherent structures exists.

Therefore a rival explanation exists, which links the non-equilibrium scaling to the co-existence of strong coherent structures with a less coherent background turbulence [16]. In the present investigation we show that in a statistical model of turbulence which does not explicitly contain coherent structures, the non-equilibrium scaling is clearly observed. We thereby show that coherent structures are not needed to explain the non-equilibrium scaling.

1.2. Objectives and outline

There are two main questions that we will address in this manuscript. The first one is whether we can reproduce the recent scaling relations of the normalised dissipation rate using the Eddy-Damped Quasi-Normal Markovian (EDQNM) closure without invoking any modification related to coherent structures. A major objective is to subtract from the dynamics the spectrum associated with perturbations around equilibrium and to show that this spectrum is proportional to $k^{-7/3}$. We will consider the case of periodically forced turbulence, since it is a well-controlled flow where the size of the fluctuations around equilibrium can be manually adjusted.

The second question is whether we can reproduce the dynamics of turbulence with non-trivial initial conditions using spectral closure. To address this question we will consider the testcase of turbulence starting from reversed initial conditions. For this, a close evaluation of the derivation of the EDQNM closure is needed, to determine how non-trivial initial conditions can be taken into account in a consistent manner. Indeed, at present, the only initial conditions which can be taken into account for simulations of developing turbulence are Gaussian initial conditions, associated with zero triple correlations, and fully developed initial conditions, associated with an established forward cascade.

In the following section we will discuss the relations which will be verified in this investigation. We also discuss the EDQNM model which allows to do so. In Section 3 the results of this investigation are presented for both periodically forced turbulence and freely evolving turbulence, starting from reversed initial conditions. Section 4 concludes this manuscript. In the appendix we will outline the EDQNM closure in a schematic manner. This will allow to determine where in the derivation the initial value of the triple correlations appears.

In this article we will explicitly show the dependence of wavenumber spectra on the wavenumber. For brevity, time and space dependence will only be explicit when their presence adds to clarity.

2. Scaling relations, test-cases and method

In the present investigation we will check the following relations,

$$C_\epsilon \sim R_\lambda^{-15/14}, \tag{2}$$

for large-scale non-equilibrium and

$$C_\epsilon \sim R_\lambda^{-2}, \tag{3}$$

for the test-case of turbulence with reversed initial conditions [17]. In these relations the Taylor-scale Reynolds number is defined as

$$R_\lambda = \sqrt{\frac{20}{3}} \frac{K}{\sqrt{\nu\epsilon}}, \tag{4}$$

with K the kinetic energy. In expression (1) the quantity U is the RMS of the longitudinal velocity fluctuations, so for an isotropic flow, $U = \sqrt{2K/3}$. The integral lengthscale is defined as

$$L = \frac{3\pi}{4K} \int k^{-1} E(k)\, \mathrm{d}k, \tag{5}$$

with $E(k)$ the energy spectrum as a function of the wavenumber k.

The main tool chosen in the present investigation to investigate the scaling relations is two-point closure theory, which we will discuss at the end of this section. We will now first define the set-ups to assess these non-equilibrium scaling relations.

2.1. Large-scale non-equilibrium

Relation (2) was derived in the limit of small perturbations around a turbulence in equilibrium. With equilibrium we mean in this context that a statistically steady state is attained where the energy injected in the flow is dissipated at the same rate. In such a flow at large Reynolds numbers a spectrum is observed (for scales at wavenumbers larger than the forcing-scale and smaller than the dissipation scale) of the form,

$$E(k,t) \sim \epsilon(t)^{2/3} k^{-5/3}, \tag{6}$$

where the average dissipation ϵ is, in such a steady state, equal to the injection rate p and energy flux. When large-scale perturbations are superposed on this system, a first-order perturbation of the Kolmogorov-scaling yields a correction of the shape [14,18,19]

$$E_1(k,t) \sim \dot{\epsilon}(t)\epsilon(t)^{-2/3} k^{-7/3}. \tag{7}$$

Using these two relations to compute the kinetic energy, dissipation and integral lengthscale lead then after some elementary algebra [13] in the limit of large Reynolds number to expression (2). Whereas (2) is observed in several flows, the scaling of the perturbation proportional to $k^{-7/3}$ has only been approximately observed in DNS of moderate Reynolds number turbulence [19]. Indeed, since E_1 is subdominant for large k, E_1 can be only observed if the equilibrium part (6) is subtracted from the instantaneous spectra. This procedure was recently also performed for the case of inhomogeneous turbulence [20].

The ideal test-case to assess the correctness of expressions (2) and (7) seems to be periodically forced turbulence [21–23], where we sustain a turbulent flow by an artificial forcing term containing a steady part plus a periodic perturbation, leading to the energy balance

$$\frac{\mathrm{d}K(t)}{\mathrm{d}t} = p_0(1 + A\cos(\omega t)) - \epsilon(t). \tag{8}$$

Periodically forced turbulence allows to consider arbitrarily small perturbations ($A \ll 1$) and arbitrary frequencies ω. It is therefore the perfect framework to assess the $-15/14$ scaling prediction since its derivation is based on perturbations around an equilibrium state.

2.2. Rapid non-equilibrium in reversed turbulence

A second type of non-equilibrium scaling was recently discovered while investigating the properties of time-reversed turbulence. It is well known that the Euler-equations are invariant under a simultaneous reversal of the velocity $\boldsymbol{u} \to -\boldsymbol{u}$ and time $t \to -t$ (see [24] for instance). This property of the Euler-equations was used in the past to assess subgrid-models for large eddy simulation [25,26]. For the Euler-equations the consequence is that, when in a flow the velocity is reversed in every point in space, the flow will evolve backwards in time until the initial condition is reached. The average direction of the energy cascade is thus reversed, which is a logical consequence of the fact that the transfer of energy is associated with triple velocity correlations, and all odd velocity correlations change sign when the velocity changes its sign.

The presence of viscous dissipation breaks this symmetry property, but nevertheless, reversing the velocity in Navier-Stokes turbulence does reverse the transfer, and the symmetry breaking by the viscous dissipation should not instantaneously affect the large scales. In Ref. [17] it was shown that such a reversal of the velocity of Navier-Stokes turbulence leads to a transfer which is heavily out-of-equilibrium giving rise to a new non-equilibrium scaling $C_\epsilon \sim R_\lambda^{-2}$. Even though reversed turbulence is a rather artificial type of flow, the same dissipation scaling is also observed in the early phase of development of certain other turbulent flows with backward energy transfer [27,28]. Clearly, this type of non-equilibrium corresponds to fast variations of the dissipation rate.

Relation (3) can be explained when the small scales vary substantially, while the large scales are almost stationary. Let us explicitly show the time-dependence of rapidly varying quantities, and let us evaluate all other quantities at instant $t = 0$. We then have

$$C_\epsilon(t) \sim \frac{\epsilon(t)L(0)}{K(0)^{3/2}} = \frac{\epsilon(0)L(0)}{K(0)^{3/2}}\frac{\epsilon(t)}{\epsilon(0)} \tag{9}$$

and

$$R_\lambda(t) \sim \frac{K(0)}{\sqrt{\nu\epsilon(0)}}\sqrt{\frac{\epsilon(0)}{\epsilon(t)}} \tag{10}$$

we find directly that,

$$\frac{C_\epsilon(t)}{C_\epsilon(0)} = \frac{\epsilon(t)}{\epsilon(0)} \quad \text{and} \quad \frac{R_\lambda(t)}{R_\lambda(0)} = \sqrt{\frac{\epsilon(0)}{\epsilon(t)}} \tag{11}$$

so that

$$C_\epsilon(t) = \left(C_\epsilon(0)R_\lambda(0)^2\right) R_\lambda(t)^{-2}. \tag{12}$$

For this scaling to be observed the large scales (determining K and L) should evolve slowly compared to the dissipation. In Ref. [17] such a system was analysed: time reversed turbulence. The main interest to consider this type of flow is not to validate the R_λ^{-2} scaling, which was well explained, but to show that closure can reproduce it. The technical point is that this necessitates to take into account non-trivial initial conditions, which is a novelty for two-point closure approaches.

2.3. Two-point closure to evaluate non-equilibrium

Since we consider unsteady isotropic turbulence, the use of two-point closure seems a suitable approach. Indeed, closures are efficient tools to study isotropic turbulence and allow to address directly ensemble averages at high Reynolds numbers. This is in particular convenient in time-dependent systems, where DNS need to be run for a substantial amount of time, or even various simulations should be carried out, to get converged statistics. Furthermore the assumptions and limitations of closure are well known so that, if a closure allows to reproduce a feature observed in DNS or experiment, we exactly know which ingredients should be taken into account to explain the phenomenon. Specifically, in the present study, since we are interested in the assessment of a sub-dominant scaling to the energy spectrum, it is valuable that the statistics we consider correspond to perfectly isotropic system. Indeed, thereby we can discard that observations are associated with anisotropy and inhomogeneity, effects which also induce subdominant corrections to the energy spectrum [20,29]. For these different reasons, closure-approaches such as the EDQNM system have played an important role in the study and understanding of turbulence since the 1970s [30–32].

We consider the evolution of the Lin-equation,

$$\partial_t E(k,t) = T(k,t) + P(k,t) - 2\nu k^2 E(k,t), \tag{13}$$

where $P(k,t)$ is a term representing the production of kinetic energy and the last term represents viscous dissipation of energy. The first term on the righthand-side, $T(k,t)$ is the nonlinear transfer term, giving rise to the transfer of energy between different scales.

For the case of large-scale non-equilibrium we force the largest scales of the system by a forcing of the form

$$P(k,t) = p_0(1 + A\cos(\omega(t))\delta(k - k_0). \tag{14}$$

where the delta-pulse is associated with a narrow band in wavenumbers at $k_0 = 1$. After a transient, the response of the turbulence becomes periodic with the same frequency ω as the forcing. During this periodic state, phase-averaged statistics are computed and instantaneous values of the integral quantities are reported. Since the transfer $T(k,t)$ integrates to zero and the viscous term to ϵ, integrating Equation (13) yields the energy balance (8).

To integrate Equation (13) the transfer term needs to be closed by a model since it contains unknown triple correlation. In the EDQNM approximation the model is given by,

$$T(k,t) = \iint_{\Delta} f_{kpq}\Theta_{kpq}(t,t_0)E(q,t)\left(\frac{E(p,t)}{p^2} - \frac{E(k,t)}{k^2}\right)\mathrm{d}p\,\mathrm{d}q, \tag{15}$$

with

$$f_{kpq} = \frac{k^2p^2}{q}(xy + z^3), \tag{16}$$

a pre-factor independent of time and Reynolds number. The integration domain Δ in the $p-q$ plane is such that triangles can be formed with sides k, p, q and x, y, z are the cosines

of the angles of this triangle [33]. The triad-timescale is given by

$$\Theta_{kpq}(t,t_0) = \frac{\left(1-(1-\alpha)\exp[L'^{(3)}_{kpq,t}(t_0-t)]\right)}{L'^{(3)}_{kpq,t}}. \tag{17}$$

with

$$L'^{(3)}_{kpq,t} = L'(k,t) + L'(p,t) + L'(q,t) \tag{18}$$

and

$$L'(k,t) = \nu k^2 + \lambda\sqrt{\int_0^k s^2 E(s,t)\,\mathrm{d}s}, \tag{19}$$

λ being a model-constant, setting the Kolmogorov constant. Here we use $\lambda = 0.5$. The technical novelty in the present investigation with respect to spectral modeling is that we can, by changing the value of α, consider a certain number of specific different initial conditions for the triple correlations. Here α can be a function of triad wavenumbers, but in the present contribution we will consider the simplest cases of constant α. Expression (17) is derived in the appendix, where it is shown that the initial transfer is associated with the value of triple correlations at t_0 when the evolution-equation for triple velocity correlations is integrated from t_0 to t. For forced steady or periodic turbulence this modification does not change the results, since the influence of the term proportional to α vanishes for $t \gg t_0$.

However at short times, in particular for the case of reversed initial conditions, this parameter is essential to take into account the influence of the initial value of the triple correlations on the transfer. Indeed, for this case, the forcing is set to zero and the turbulence is left to decay freely. We start from a normally decaying case (*i.e.*, $\alpha = 0$) and wait until C_ϵ is quasi constant, which corresponds to fully developed triple correlations. Subsequently we change α to consider reversed initial conditions.

3. Results

In this section we present the results of the two considered test-cases. First we show the results for turbulence submitted to time-periodic forcing. Then we will show the case of reversed initial conditions. In both cases we will focus on the non-equilibrium properties, as characterised by the behavior of the normalised dissipation rate.

The closure implementation is basically unchanged over the decades and the code is similar to the one described in [31,32,34] using a routine developed in Ref. [35]. The main difference is that, whereas in the 1970s super-computing facilities were needed, the integration is now carried out at higher resolution and higher Reynolds numbers using a simple laptop.

3.1. Spectral imbalance in periodically forced turbulence

We consider an isotropic turbulent flow, maintained by forcing protocol (14) containing both a steady and a periodic contribution. The spectral grid ranges from $k = 1$ to $k\eta \approx 5$ (with $\eta = \nu^{3/4}\epsilon^{-1/4}$) using typically 100-200 gridpoints, logarithmically spaced.

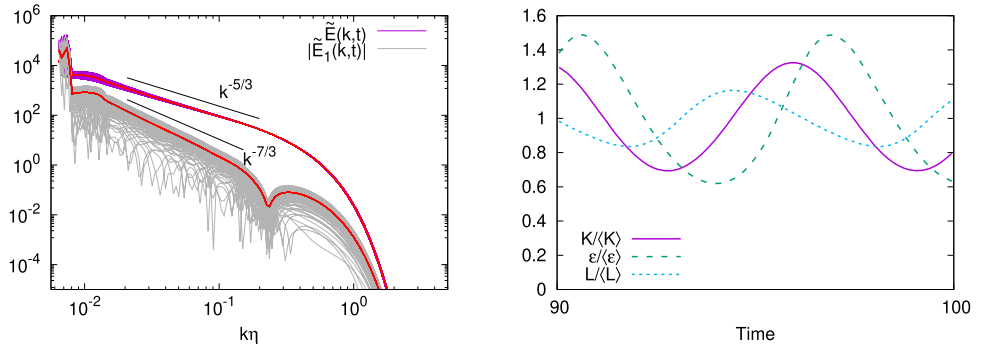

Figure 1. Results for $\langle R_\lambda \rangle = 240$, modulation amplitude $A = 1$ and $\omega T = 1$. (a) Kolmogorov-normalised energy spectra. The violet lines indicate $\tilde{E}(k,t) \equiv E(k,t)\epsilon^{-1/4}\nu^{-5/4}$ as a function of time. The grey lines correspond to the absolute value of the energy spectra $|\tilde{E}_1(k,t)| \equiv |E_1(k,t)|\epsilon^{-1/4}\nu^{-5/4}$ associated with the temporal perturbation. Averaged spectra are shown in red. (b) Associated time-series of K, ϵ, L during the statistically steady state.

CPU-time is approximately 1 minute per computation up to $t = 100$, on a regular desktop computer or laptop. The viscosity is first set at $\nu = 0.001$ resulting in an average Reynolds number of $\langle R_\lambda \rangle \approx 240$ but for larger values of the Reynolds number the dynamics do not significantly change as we will illustrate. The value of the mean energy input rate is set to $p_0 = 0.35$. The values of A and ω determine the amplitude and frequency of the modulation, respectively. For the modulation frequency first results are presented for $\omega T = 0.5; 1; 2$, with $T = L/U \approx 1$. This corresponds to a modulation with a frequency around the natural frequency of the turbulence.

We report results for two amplitudes. The former, $A = 1$ represents modulation of the energy input with fluctuations of the order of the mean input rate, whereas the second value, $A = 0.1$ allows to consider the modulation as a small periodic perturbation upon the steady flow. A detailed investigation of periodically forced turbulence, in particular its amplitude response, was carried out using the same set-up [23].

In Figure 1(a) we show the kinetic energy spectrum for different time-instants for the case $A = 1$ and $\omega T = 1$. The average Reynolds number is large enough to observe the beginning of an inertial range with a scaling proportional to $k^{-5/3}$.

The spectra are time-averaged over a cycle of the forcing for every value of $k\eta$ (note that a linear interpolation is used to transpose the spectra from a k-grid to a $k\eta$-grid), to obtain the equilibrium spectrum. This equilibrium spectrum is shown in red. Only at small $k\eta$ values the instantaneous spectra can be visually distinguished from the average in this representation.

Subtracting the equilibrium spectrum from the instantaneous energy spectra yields the perturbation spectrum (see also [20]). This spectrum is a highly fluctuating quantity, since it can be both positive and negative. Nevertheless, the average of the absolute value allows to show the onset of the $k^{-7/3}$ spectrum, in agreement with the theoretical prediction (7) and confirming the low Reynolds observations ($R_\lambda \approx 120 - 140$) in DNS [19]. Note that the scaling range is not well developed here and the wavenumber dependence not perfectly

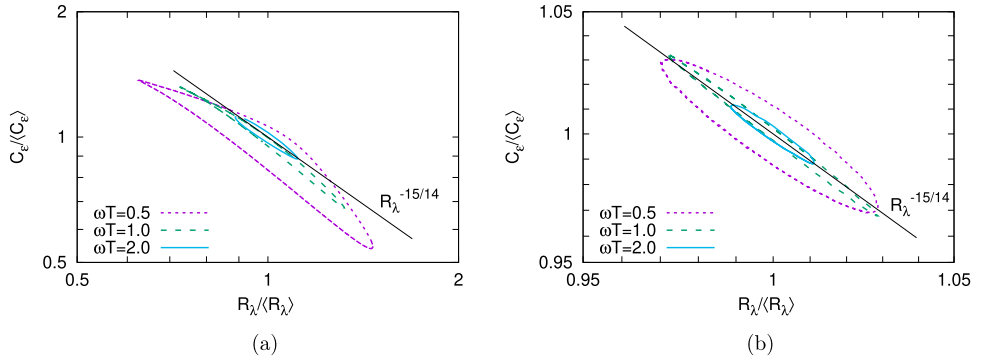

Figure 2. Parametric plot of C_ϵ as function of R_λ during the statistically steady state at $\langle R_\lambda \rangle = 240$. (a) Modulation amplitude $A = 1$. (b) Modulation amplitude $A = 0.1$.

proportional to $-7/3$. This will be further examined at higher values of the Reynolds number below.

In Figure 1(b) we show the temporal signals of the main quantities for the case of $A = 1$ and $\omega T = 1$, normalised by their time-averaged values. A phase-shift is observed between the different quantities. For a detailed analysis and explanation of the origin of these phase shifts we refer to [23]. Results for the spectra for $A = 0.1$ are very similar and are not shown.

From these three quantities K, ϵ, L we can compute the normalised dissipation rate C_ϵ and the Reynolds number. The parametric plot of these quantities is shown in Figure 2 for different amplitudes and frequencies. Both quantities are normalised by their time-averages. The value for the average normalised dissipation rate is $\langle C_\epsilon \rangle = 0.42$.

The results for amplitude $A = 1$ and $A = 0.1$ are shown in Figure 2(a-b) respectively. The qualitative behavior is fairly similar with all plots being approximately aligned with the theoretical $R_\lambda^{-15/14}$ scaling. These results are also consistent with the DNS results of Ref. [11] where the modulation is not imposed, but is a natural consequence of the turbulent dynamics. The amplitudes of the excursions around the average values are determined by the amplitude of the modulation, as is illustrated by comparing the two plots in Figure 2(a-b). Also the amplitudes in these parametric plots decrease for higher frequencies, which is a consequence of the exact frequency dependence of the amplitudes of the different quantities [23]. A persistent feature for all plots is the elliptic shape of the curves. This feature needs further examination.

It is interesting to assess how robust the dissipation scaling is as a function of the modulation frequency. At high frequencies $\omega T \gg 1$ the variations of the integral quantities become infinitesimally small. In this limit only the forced mode is affected by the modulation [23]. In this limit the dissipation scaling is not expected to hold, since it assumes a broad-band perturbation spectrum and not a spectrum restricted to the forced modes only. In this limit the perturbations do therefore vanish and should not necessarily satisfy the $-15/14$ scaling.

At very low frequencies $\omega T \ll 1$, the turbulence behaves in a quasi-static manner and the perturbation spectrum should become infinitesimally small. However, the slowly varying integral scales should lead to a slowly varying Reynolds number. In this limit the value

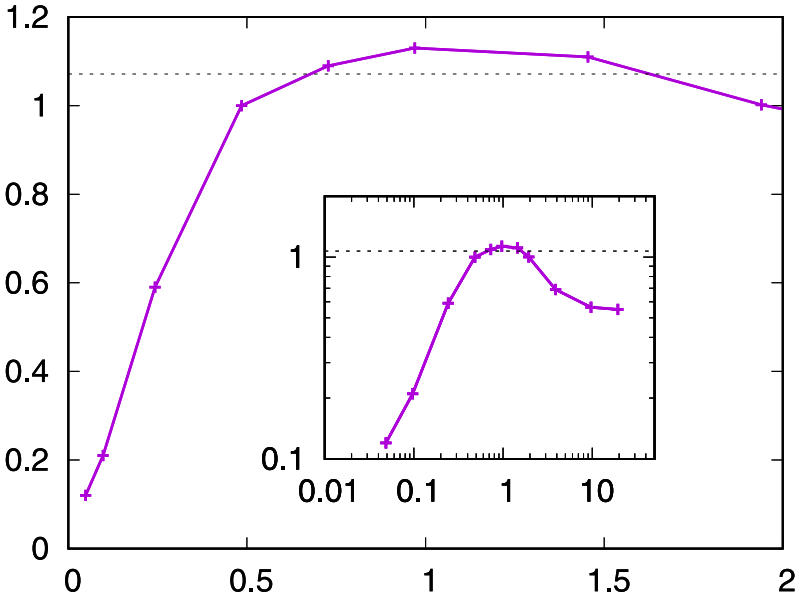

Figure 3. Scaling of the exponent n in the relation $C_\epsilon \sim R_\lambda^{-n}$ as a function of the modulation frequency during the statistically steady state at $\langle R_\lambda \rangle = 240$ and modulation amplitude $A = 1$. The dashed line represents the value 15/14. The inset shows the data in double-logarithmic representation.

of C_ϵ should therefore remain constant, while R_λ varies. The exponent n in $C_\epsilon \sim R_\lambda^{-n}$ should thus go to zero.

We have systematically changed the frequency in the range $\omega T \in [0.01, 20]$ and the results of the exponent n is shown in Figure 3. The exponent is determined as a best fit of a power law to the data during the steady-state. The low frequency 'quasi-static' limit $n = 0$ is observed. At high frequencies, in the 'rapid-distortion' limit $\omega T \gg 1$ the exponent drops from the theoretical scaling towards a value close to 0.5. The range of frequencies where the theoretical value is approached is situated around $\omega T = 1$.

One could argue that this range is relatively small. However, it should be realised that this is the most important range of frequencies. Indeed, in most flows we cannot simply decompose the flow into a mean-forcing plus a modulation, since both are in general generated by the same physical effects. The turbulence does then act as a whole and the time-scale on which it acts is the integral frequency. Furthermore, it was shown experimentally that to affect the turbulence, and in particular its dissipation rate, the most efficient stirring frequency is associated with the integral timescale [36]. The frequency $\omega T \approx 1$ is thus the important reference case for all natural evolving turbulent flows, such as wake, grid or jet-flows, and this is where the dissipation scaling (2) holds. Stirring turbulence at a length scale with a modulation frequency which is too distinct from the typical turbulent timescale associated with that length scale is not efficient. This is clearly illustrated in [23], where it is shown that for high frequencies the response of the kinetic energy and dissipation decays rapidly. If one wants to stir or affect the turbulence at a more rapid timescale, one needs not act only on the large scales but also at the small, more rapidly evolving scales.

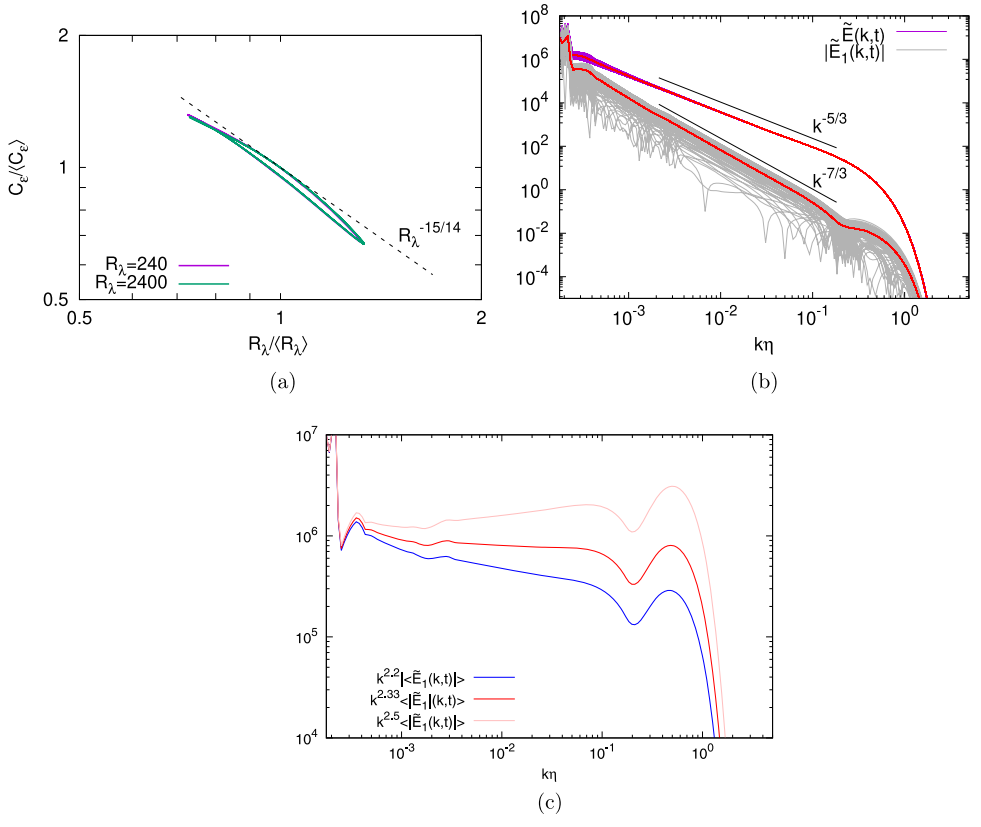

Figure 4. (a) Parametric plot of C_ϵ as function of R_λ during the statistically steady state comparing $\langle R_\lambda\rangle = 240$ and 2400. Modulation amplitude $A = 1$, $\omega T = 1$. (b) Energy spectra at $\langle R_\lambda\rangle = 2400$. Kolmogorov normalised energy spectra $\tilde{E}(k,t) \equiv E(k,t)\epsilon^{-1/4}\nu^{-5/4}$ as a function of time and absolute value of the energy spectra $\tilde{E}_1(k,t) \equiv E_1(k,t)\epsilon^{-1/4}\nu^{-5/4}$ associated with the temporal perturbation. Averaged spectra are shown in red. (c) Compensated plots $k^m\langle\tilde{E}_1(k,t)\rangle$ for three values of m.

This is exactly the case in reversed turbulence (considered in the next section), where not only the large scales are affected but also directly the rapidly evolving dissipation-scales.

A remaining question is whether the results change at higher values of the Reynolds number. In order to assess this, we have carried out a numerical integration at a value of an order of magnitude larger, i.e. at $R_\lambda \approx 2400$. In Figure 4(a) we compare the $C_\epsilon(R_\lambda)$ plots at $R_\lambda = 240$ and 2400. It is observed that the results practically collapse. This illustrates that the results are governed by the large energy containing scales, as anticipated [13].

Furthermore, in Figure 4(b) we show the energy-spectra $E(k,t)$ as a function of time. As for the $R_\lambda = 240$ results, we observe that in Kolmogorov-units these spectra almost perfectly collapse at high values of k. Again substracting this equilibrium spectrum from the energy spectra yields an estimate for the spectrum $E_1(k,t)$ associated with the perturbation. The $k^{-7/3}$ scaling is observed over a wavenumber interval spanning more than two decades. To more precisely determine the powerlaw dependence, we show in Figure 4(c) compensated spectra. It is observed that the powerlaw exponent is close to $-7/3$ in the inertial range. However, near the forcing scale the spectrum is significantly steeper.

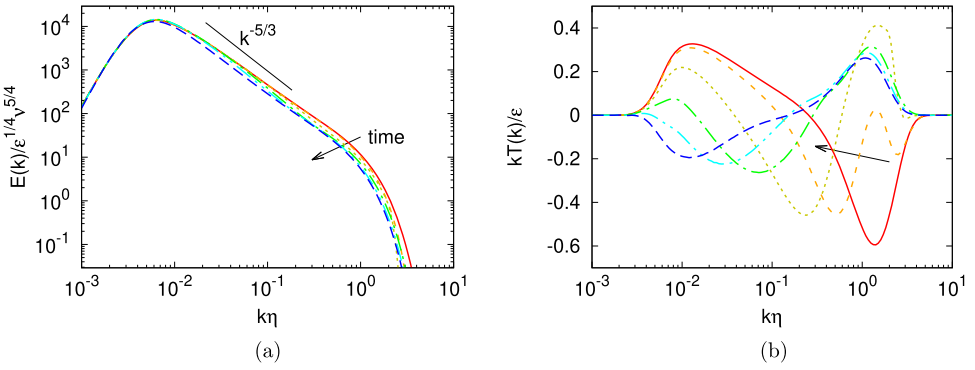

Figure 5. (a) EDQNM results for the evolution of kinetic energy spectra. (b) Evolution of the nonlinear transfer spectrum. The arrows in each figure denotes the time direction.

The conclusion of this part is that in periodically forced turbulence the theoretically predicted scaling for the normalised dissipation rate is observed for stirring frequencies around the frequency of the most energetic structures of turbulence, which is the natural frequency on which most global features of a flow evolve. When the stirring frequency deviates far enough from the integral frequency, the scaling does also change, as expected. An additional conclusion is that no coherent structures need to be present to produce the non-equilibrium scaling. Furthermore, the non-equilibrium spectra is shown to scale proportional to $k^{-7/3}$, in agreement with theory.

3.2. *Rapid non-equilibrium in reversed turbulence*

We now turn to the results for freely evolving turbulence where the transfer is reversed. The turbulence starts from Gaussian initial conditions and is left to decay. Once a self-similar decay is observed with a close to constant normalised dissipation rate, the transfer is reversed by setting $\alpha = -1$ in expression (17). At this time the Reynolds number is $R_\lambda = 253$.

The energy spectra at several time instants are shown in Figure 5. During a short time-interval, the velocity reversal leads to a backward energy transfer, that is, decrease of small-scale energy and increase of large-scale energy.

The associated energy transfer spectra at the same time-instants are shown in Figure 5(b). It is observed that initially $T(k)$ is positive at lower wavenumbers while negative at higher wavenumbers, indicating a reversed transfer. This evolves gradually to a forward transfer. The important observation in this figure is therefore that we can reproduce reversed turbulence using EDQNM, which opens the way to study the effect of non-trivial initial conditions for the energy transfer using EDQNM.

The next question we ask is whether we confirm the non-equilibrium scaling (3). We plot the associated quantities in Figure 6 and show that indeed, the -2 scaling is very clearly observed. In this early stage of the simulation, the Reynolds number increases, since the large scale structures change slowly (leading to quasi constant kinetic energy K and integral lengthscale L) but small scales change rapidly (leading to unsteady dissipation ε). Then

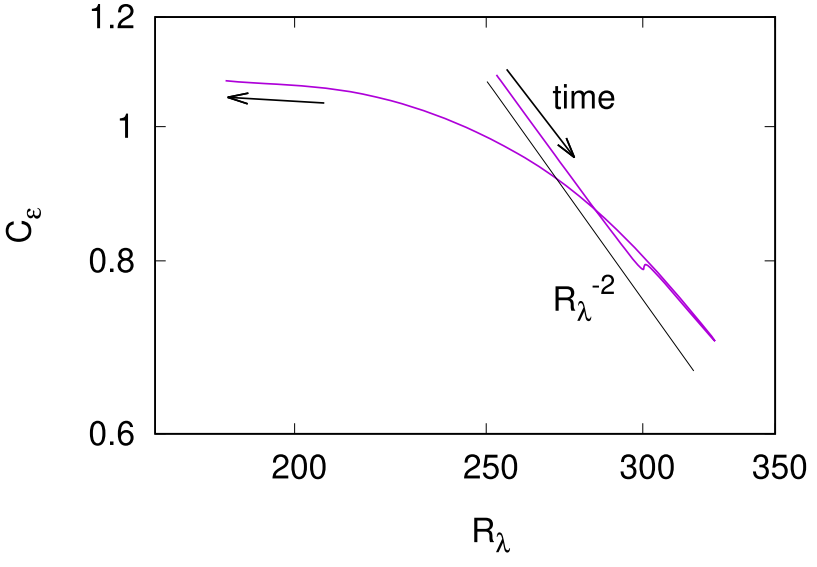

Figure 6. Relation between C_ε and Re_λ, by using modified EDQNM with reversed initial field. The arrow in each figure denotes the time direction.

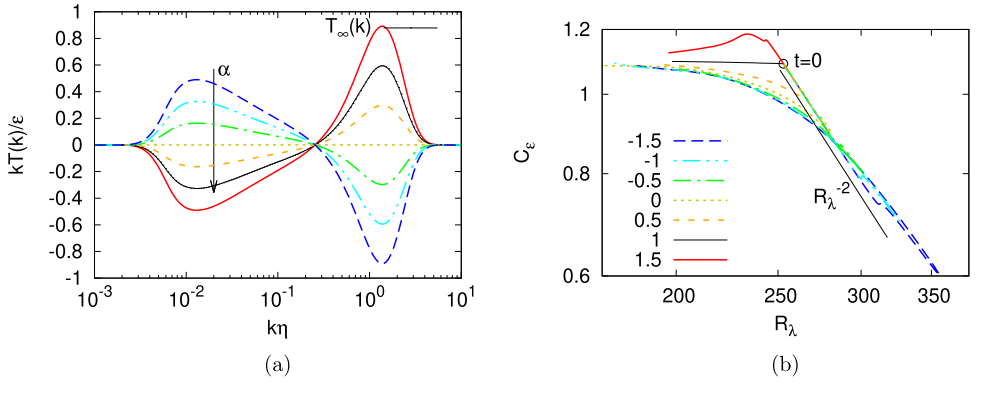

Figure 7. (a) Initial nonlinear transfer spectra for different EDQNM cases. The vertical arrow indicates the increase of α from -1.5 to 1.5 respectively. (b) Relation between C_ε and Re_λ, for the cases illustrated in (a).

after a transition stage, the flow field is self-organised and freely decays with quasi constant C_ε. This thus provides evidence that the observations in [17] are robust enough to be reproduced using spectral closure theory.

To somewhat further investigate the influence of initial conditions on the dissipation-rate scaling, we perform a parametric study where we vary in expression (17) for the triad-timescale the value of the parameter α in the range $\alpha \in [-1.5, 1.5]$. Several values of α are associated with specific physical situations: $\alpha = -1$ corresponds to reversed turbulence, $\alpha = 0$ to Gaussian (zero triple correlation) velocity modes and $\alpha = 1$ to developed turbulence. Initial energy transfer spectra are shown in Figure 7(a). All cases share the same energy spectrum with different initial transfers. Specifically, the transfer $T_\infty(k)$ marked in

Figure 7(a) corresponds to the transfer predicted by traditional EDQNM procedures at the long-time limit. In Figure 7(b) it is observed that all parametric plots start at the same position for $t = 0$. At long times they all tend to the asymptotic value $C_\epsilon \approx 1.1$. The case with $\alpha = 1$ starts directly on this asymptotic value.

All other cases evolve initially along the R_λ^{-2} relation. The maximum deviation from the asymptotic value is importantly influenced by the value of α, with all values $\alpha < 1$ leading to negative deviations and the $\alpha > 1$ case leading to a positive deviation. All these systems are thus affected at the small scales and confirm the R_λ^{-2} small scale non-equilibrium relation.

4. Conclusion

We have focused in this work on temporal fluctuations of the normalised dissipation rate. We have shown that the dissipation-rate scaling relations Equations (2) and (3) are observable in two-point closure simulations of isotropic turbulence. For the case of periodically forced turbulence, the parametric plots $(R_\lambda(t), C_\epsilon(t)$ show an elliptic shape with a longer-axis proportional to $R_\lambda^{-15/14}$.

This shows that coherent structures are no prerequisite to have these types of non-equilibrium turbulence. Also, we report on the first high Reynolds number confirmation of a $k^{-7/3}$ spectrum associated with unsteady perturbations around equilibrium, confirming theoretical arguments and low Reynolds number DNS results [19]. Furthermore, we showed that non-trivial initial conditions for triple correlations can be specified in the framework of the EDQNM closure. Thereby reversed turbulence can be investigated by closure.

Even though we stressed that all these observations are reminiscent of situations where the turbulence is out of equilibrium, we should admit that C_ϵ remains a rather robust quantity. In all the flows considered here, be it forced by a large-amplitude periodic energy input, or starting from reversed initial conditions, the value of C_ϵ remains bounded. Indeed, for the periodically forced cases, the value of C_ϵ varies between $0.2 < C_\epsilon < 0.6$, whereas in the freely evolving case its value varies between 0.6 and 1.2. This relative robustness is certainly reassuring for the use of turbulence models which heavily rely on the approximate constant value of the normalised dissipation. It will depend on the application whether the amount of non-equilibrium should be taken into account. For flows exhibiting large values of the non-equilibrium, 2−equation models might be not precise enough and models using more degrees of freedom should be preferred [15,37,38].

Acknowledgements

The book 'turbulence in fluids' by Marcel Lesieur [39] has played an essential role in the understanding of turbulence of one of the authors. It has accompanied WB during his carreer and the pages of chapter VII on EDQNM have all detached from their bindings. The code used in this work to integrate the EDQNM equations is practically the same as the one Marcel Lesieur and his colleagues used since the 1970s.

LF is supported by the Science Center for Gas Turbine Project (Project No. P2022-C-III-001-001). For the purpose of Open Access, a CC-BY public copyright licence has been applied by the authors to the present document and will be applied to all subsequent versions up to the Author Accepted Manuscript arising from this submission.

Disclosure statement

No potential conflict of interest was reported by the author(s).

ORCID

Wouter J.T. Bos http://orcid.org/0000-0003-3510-0362

References

[1] Taylor GI. Statistical theory of turbulence. Proc R Soc London Ser A, Math Phys Sci. 1935;151:421–444.
[2] Rubinstein R, Clark TT. 'Equilibrium' and 'non-equilibrium' turbulence. Theoretical Appl Mech Lett. 2017;7:301–305.
[3] Sreenivasan KR. On the scaling of the turbulence energy dissipation rate. Phys Fluids. 1984;27:1048.
[4] Pearson BR, Krogstad PA, van de Water W. Measurements of the turbulent energy dissipation rate. Phys Fluids. 2002;14:1288.
[5] Burattini P, Lavoie P, Antonia RA. On the normalised turbulent energy dissipation rate. Phys Fluids. 2005;17:098103.
[6] Bos WJT, Shao L, Bertoglio JP. Spectral imbalance and the normalised dissipation rate of turbulence. Phys Fluids. 2007;19:045101.
[7] Goto S, Vassilicos JC. The dissipation rate coefficient of turbulence is not universal and depends on the internal stagnation point structure. Phys Fluids. 2009;21:035104.
[8] Seoud RE, Vassilicos JC. Dissipation and decay of fractal-generated turbulence. Phys Fluids. 2007;19:105108.
[9] Valente PC, Vassilicos JC. Universal dissipation scaling for nonequilibrium turbulence. Phys Rev Lett. 2012;108:214503.
[10] Hearst RJ, Lavoie P. Decay of turbulence generated by a square-fractal-element grid. J Fluid Mech. 2014;741:567–584.
[11] Goto S, Vassilicos JC. Energy dissipation and flux laws for unsteady turbulence. Phys Lett A. 2015;379:1144–1148.
[12] Meldi M, Sagaut P. Investigation of anomalous very fast decay regimes in homogeneous isotropic turbulence. J Turbulence. 2018;19:390–413.
[13] Bos WJT, Rubinstein R. Dissipation in unsteady turbulence. Phys Rev Fluids. 2017;2:022601.
[14] Yoshizawa A. Nonequilibrium effect of the turbulent-energy-production process on the inertial-range energy spectrum. Phys Rev E. 1994;49:4065.
[15] Bos WJT. Production and dissipation of kinetic energy in grid turbulence. Phys Rev Fluids. 2020;5:104607.
[16] Goto S, Vassilicos J. Unsteady turbulence cascades. Phys Rev E. 2016;94:053108.
[17] Liu F, Lu L, Bos WJ, et al. Assessing the nonequilibrium of decaying turbulence with reversed initial fields. Phys Rev Fluids. 2019;4:084603.
[18] Rubinstein R, Clark T, Livescu D, et al. Time-dependent isotropic turbulence. J Turbul. 2004;5:011.
[19] Horiuti K, Tamaki T. Nonequilibrium energy spectrum in the subgrid-scale one-equation model in large-eddy simulation. Phys Fluids. 2013;25:125104.
[20] Araki R, Bos WJT. Inertial range scaling of inhomogeneous turbulence. preprint arXiv:2210.14516, 2022.
[21] Lohse D. Periodically kicked turbulence. Phys Rev E. 2000;62:4946.
[22] Kuczaj AK, Geurts BJ, Lohse D. Response maxima in time-modulated turbulence: direct numerical simulations. Europhys Lett. 2006;73:851.
[23] Bos WJT, Clark T, Rubinstein R. Small scale response and modeling of periodically forced turbulence. Phys Fluids. 2007;19:055107.
[24] Orszag SA. Lectures on the statistical theory of turbulence.New York : Flow Research Inc.; 1974.

[25] Carati D, Winckelmans G, Jeanmart H. On the modelling of the subgrid-scale and filtered-scale stress tensors in large-eddy simulation. J Fluid Mech. 2001;441:119.
[26] Fang L, Bos WJT, Shao L, et al. Time reversibility of Navier-Stokes turbulence and its implication for subgrid scale models. J Turbul. 2012;13:N3.
[27] Liu F, Fang L, Fang J. Non-equilibrium turbulent phenomena in transitional flat plate boundary-layer flows. Appl Math Mech. 2021;42:567–582.
[28] Zhao H, Liu Y, Shao L, et al. Existence of positive skewness of velocity gradient in early transition. Phys Rev Fluids. 2021;6:104608.
[29] Lumley J. Similarity and the turbulent energy spectrum. Phys Fluids. 1967;10:855.
[30] Orszag SA. Analytical theories of turbulence. J Fluid Mech. 1970;41:363.
[31] André J, Lesieur M. Influence of helicity on the evolution of isotropic turbulence at high Reynolds number. J Fluid Mech. 1977;81:187.
[32] Lesieur M, Schertzer D. Amortissement auto-similaire d'une turbulence à grand nombre de Reynolds. J Mécanique. 1978;17:609–646.
[33] Leslie D. Developments in the theory of turbulence. Oxford: Oxford University Press; 1973.
[34] Pouquet A, Lesieur M, André J, et al. Evolution of high Reynolds number two-dimensional turbulence. J Fluid Mech. 1975;72:305–319.
[35] Leith C. Atmospheric predictability and two-dimensional turbulence. J Atmos Sci. 1971;28:145–161.
[36] Cekli H, Tipton C, van de Water W. Resonant enhancement of turbulent energy dissipation. Phys Rev Lett. 2010;105:044503.
[37] Schiestel R. Multiple-time-scale modeling of turbulent flows in one-point closures. Phys Fluids. 1987;30:722.
[38] Cadiou A, Hanjalić K, Stawiarski K. A two-scale second-moment turbulence closure based on weighted spectrum integration. Theoretical Comput Fluid Dyn. 2004;18:1–26.
[39] Lesieur M. Turbulence in fluids. Dordrecht: Kluwer Dordrecht; 1990.
[40] Sagaut P, Cambon C. Homogeneous turbulence dynamics. Cambridge: Cambridge University Press; 2008.

Appendix. The EDQNM closure with particular focus on time dependence

The derivation of the EDQNM model is now quite standard [24,39,40]. We will recall the derivation in symbolic notation here focusing on particular on the time-dependence of damping terms and the memory of initial conditions. Before introducing symbolic notation, we show the Fourier-representation of Navier-Stokes turbulence and the resulting unclosed equations for second order correlations. These are for the Navier-Stokes equations,

$$\partial_t u_i(\boldsymbol{k},t) = -L(\boldsymbol{k},t)u_i(\boldsymbol{k},t) - ik_j P_{im}(\boldsymbol{k}) \int \delta(\boldsymbol{k}-\boldsymbol{p}-\boldsymbol{q}) u_j(\boldsymbol{p},t) u_m(\boldsymbol{q},t)\, \mathrm{d}\boldsymbol{p}\, \mathrm{d}\boldsymbol{q}, \tag{A1}$$

with

$$P_{im}(\boldsymbol{k}) = \left(\delta_{im} - k_i k_m / k^2\right) \tag{A2}$$

and the term $L(\boldsymbol{k},t)$ is

$$L(\boldsymbol{k},t) = \nu k^2 - F(k,t). \tag{A3}$$

Here ν is the kinematic viscosity and $F(k,t)$ determines the shape of the forcing spectrum. Multiplying by $u_i(-\boldsymbol{k},t)$ and averaging yields for the velocity-auto-correlation, $U(k,t) = \langle u_i(\boldsymbol{k},t) u_i(-\boldsymbol{k},t)\rangle$,

$$\partial_t U(k,t) = -[L(\boldsymbol{k},t) + L(-\boldsymbol{k},t)]U(k,t) - iP_{ijm} \int \delta(\boldsymbol{k}-\boldsymbol{p}-\boldsymbol{q}) \langle u_j(\boldsymbol{p},t) u_m(\boldsymbol{q},t) u_i(-\boldsymbol{k},t)\rangle\, \mathrm{d}\boldsymbol{p}\, \mathrm{d}\boldsymbol{q}. \tag{A4}$$

with $P_{ijm}(\boldsymbol{k}) = k_j P_{im}(\boldsymbol{k}) + k_m P_{ij}(\boldsymbol{k})$. Similarly, an equation can be derived for the triple correlations on the RHS of Equation (A4).

We write these equations in symbolic notation,

$$\frac{\partial u}{\partial t} = -L^{(1)}u + F^{(1)}[uu] \tag{A5}$$

$$\frac{\partial \langle uu\rangle}{\partial t} = -L^{(2)}\langle uu\rangle + F^{(2)}[\langle uuu\rangle] \tag{A6}$$

$$\frac{\partial \langle uuu\rangle}{\partial t} = -L^{(3)}\langle uuu\rangle + F^{(3)}[\langle uuuu\rangle] \tag{A7}$$

where all indices, integrals and time and wave-vector dependencies are omitted. Equations (A5) and (A6) are symbolic representations of Equations (A1) and (A4), respectively.

Classically, the next step is invoking the quasi-normal assumption, where all fourth-order correlations are expressed as a function of second order correlations. This is represented by $\langle uuuu\rangle \rightarrow \Sigma\langle uu\rangle\langle uu\rangle$. The procedure is called quasi-Normal, since in a fully normal system, the triple correlations would also be Gaussian and thereby zero. To improve upon the performance of the quasi-Normal closure, eddy damping is added to the linear term of the triple correlations,

$$L^{(3)} \rightarrow L^{(3)} + \eta(k) + \eta(p) + \eta(q) \equiv L'^{(3)}, \tag{A8}$$

yielding

$$\frac{\partial \langle uuu\rangle}{\partial t} = -L'^{(3)}\langle uuu\rangle + F^{(3)}[\Sigma\langle uu\rangle\langle uu\rangle]. \tag{A9}$$

Equation (A9) can be integrated, yielding

$$\langle uuu\rangle = \exp\left(-\int_{t_0}^{t} L'^{(3)}(t')\,\mathrm{d}t'\right) \times \left[\int_{t_0}^{t}\left\{\exp\left(\int_{t_0}^{t'} L'^{(3)}(t'')\,\mathrm{d}t''\right)F^{(3)}[\Sigma\langle uu\rangle(t')\langle uu\rangle(t')]\right\}\mathrm{d}t' + \langle uuu\rangle_0\right], \tag{A10}$$

where $\langle uuu\rangle_0$ appears as an integration constant, determined by the initial conditions of the triple correlations. The last step in the EDQNM approximation allowing to obtain a simple closed expression for the evolution of the triple correlations is the Markovianization. This procedure assumes that the triple correlations are the quantities which are most rapidly varying in time. Assuming L' and $\langle uu\rangle$, which both depend on time t, constant compared to the exponential, the expression becomes

$$\langle uuu\rangle = \exp[-L'^{(3)}t]\left[\int_{t_0}^{t}\exp[L'^{(3)}t']\,\mathrm{d}t' F^{(3)}[\Sigma\langle uu\rangle(t)\langle uu\rangle(t)] + \langle uuu\rangle_0\right]. \tag{A11}$$

We can integrate the last expression to find.

$$\langle uuu\rangle = \Theta' F^{(3)}[\Sigma\langle uu\rangle\langle uu\rangle] + \langle uuu\rangle_0 \exp[-L'^{(3)}t], \tag{A12}$$

with

$$\Theta' = \frac{\left(1 - \exp[L'^{(3)}(t_0 - t)]\right)}{L'^{(3)}}. \tag{A13}$$

The important point for the present investigation is the presence of the last term in (A12), resulting from the integration constant $\langle uuu\rangle_0$. The EDQNM closure can thus not be integrated as long as the initial value of the triple correlations is unknown. Determining this quantity is not straightforward since it corresponds to a correlation among three Fourier modes. Experimentally determining this correlation seems excessively complicated. The common procedure in most closure investigations of freely evolving turbulence is therefore to add an assumption on the initial conditions. There are two obvious choices. The first one is to assume that the initial conditions are Gaussian, assuming

zero value $\langle uuu\rangle_0 = 0$. The second choice is to assume that the initial field is fully developed, so that

$$\langle uuu\rangle_0 = \frac{\exp[L'^{(3)}t_0]}{L'^{(3)}} F^{(3)}[\Sigma\langle uu\rangle\langle uu\rangle]. \tag{A14}$$

This particular choice leads to the expression for the triple correlations,

$$\langle uuu\rangle = \Theta F^{(3)}[\Sigma\langle uu\rangle\langle uu\rangle], \tag{A15}$$

with

$$\Theta = \frac{1}{L'^{(3)}}. \tag{A16}$$

A third choice for the triple correlations, which is of particular interest for the present study, consists in assuming the flow developed, but with reversed initial conditions, this would correspond to

$$\langle uuu\rangle_0 = -\frac{\exp[L'^{(3)}t_0]}{L'^{(3)}} F^{(3)}[\Sigma\langle uu\rangle\langle uu\rangle], \tag{A17}$$

leading to the triple correlation time,

$$\Theta = \frac{\left(1 - 2\exp[L'^{(3)}(t_0 - t)]\right)}{L'^{(3)}}. \tag{A18}$$

We can generalise these three possibilities by the following expression:

$$\Theta = \frac{\left(1 - (1-\alpha)\exp[L'^{(3)}(t_0 - t)]\right)}{L'^{(3)}}. \tag{A19}$$

However these possibilities are not exhaustive since we have assumed here that the initial transfer is proportional to the developed transfer at every wavenumber. A more general expression can be imagined if other cases need to be considered, but expression (A19) is sufficiently general for the present investigation.